Available online at www.sciencedirect.com
ScienceDirect
Journal of the European Ceramic Society 30 (2010) 917–926
www.elsevier.com/locate/jeurceramsoc

# Dispersant-free colloidal fabrication of $Bi_2Sr_2CaCu_2O_8$ superconducting thick films

M. Mora [a,*], F. Gimeno [a], H. Amaveda [a], L.A. Angurel [a], R. Moreno [b]

[a] *Instituto de Ciencia de Materiales de Aragón (CSIC-Universidad de Zaragoza), C/ María de Luna 3, 50018 Zaragoza, Spain*
[b] *Instituto de Cerámica y Vidrio - CSIC, C/ Kelsen, 5, 28049 Madrid, Spain*

Received 14 May 2009; received in revised form 8 October 2009; accepted 22 October 2009
Available online 24 November 2009

**Abstract**

$Bi_2Sr_2CaCu_2O_x$ thick films have been fabricated using colloidal processing. The composition of the suspension has been optimised using sedimentation experiments and rheological measurements. It has been stated that well-dispersed suspensions of $Bi_2Sr_2CaCu_2O_x$ can be obtained when ethanol is used as a solvent without the addition of deflocculants. Using the fits of the viscosity curves to the Krieger–Dougherty model, it has been possible to determine that the maximum volume fraction of solids leading to stable suspensions is 0.37. With these suspensions, it has been possible to fabricate films with 130 μm in thickness that show enough resistance to cracking and allow easy handling. Superconducting coatings have been obtained without dispersant.
Published by Elsevier Ltd.

*Keywords:* Suspensions; Tape casting; Oxide superconductors; Rheology

## 1. Introduction

Colloidal processing is a usual pathway for preparing superconducting $Bi_2Sr_2CaCu_2O_x$ (Bi-2212) thick films which includes dip coating,[1,2] screen-printing,[3] tape casting[4,5] or electrophoretic deposition.[6] All these techniques use specific organic additives to obtain adequate slurry. The composition of this slurry depends on the requirements of the particular processing techniques. This is more evident in the case of tape casting, where a more sophisticated preparation procedure has to be used.

Tape casting is selected as a suitable processing technique for many applications due to the possibility of obtaining self-supporting films with a precise control of the thickness whose width is only limited by the blade dimensions. It requires the preparation of stable slurry of ceramic powder in a liquid medium. Ceramic powders tend to agglomerate in the suspension due to attractive van der Waals forces. To overcome them, the addition of an appropriate dispersant is necessary to assure the suspension stability. Usually, tape casting slurries contain other organic additives such as a binder and a plasticizer to obtain optimum strength and flexibility values.

After being prepared, the suspension is deposited on a flat surface and levelled through the action of a blade. After drying, samples are cut from the green tape and put onto the substrates if it is necessary. Finally, organic additives are removed with a heat treatment and samples are consolidated by an adequate thermal treatment at the sintering temperature.

In the case of Bi-2212 thick films, superconducting properties are strongly related with the sample texture, which can be induced by a partial melt process at temperatures higher than the solidus one followed by slow cooling to the sintered temperature.[4] Besides partial melting process, the Laser Zone Melting (LZM) method has been used as a suitable technique to texture this superconducting material in a planar configuration. Recently, Bi-2212 thick films were obtained on (1 0 0) MgO substrates by combining both, tape casting and LZM techniques.[7] However, the LZM process is very sensitive to the green tape characteristics, strongly determined by the quality of the slurry. In particular, the solid loading must be high enough in order to avoid the "beading" effect observed in some cases in these materials[7,8] with periodic width and thickness variations in the solidified material.

* Corresponding author. Tel.: +34 976 761 958; fax: +34 976 761 957.
*E-mail address:* mmora@unizar.es (M. Mora).

0955-2219/$ – see front matter. Published by Elsevier Ltd.
doi:10.1016/j.jeurceramsoc.2009.10.018

Solid loading can be increased by optimizing the amount of the dispersant that has to be added into the suspension. It depends on different powder characteristics such as the specific surface area or the particle size distribution. Therefore, for each particular system the amount of all additives has to be carefully optimized with respect to slip viscosity and green tape properties. In addition, the choice of the dispersant is very important because it should not contaminate the final product. To obtain an appropriated slurry with superconducting Bi-2212 powders, Glycerol Trioleate (Triolein)[4,5,9] or Sorbitan Trioleate[1,7,10,11] have been normally used as dispersant. In other cases, Terpineol has been added to the slurry. However, it is not clear if this compound acts as a dispersant or as a solvent.[12,13]

The suspension stability depends not only on the dispersant but also on the solvent. Ethanol is the most common solvent chosen for different ceramic suspensions because it does not adversely affect the powder, dissolves most of the organic additives and has a very good balance considering different properties as drying rate, cost, dielectric constant or surface tension. In fact, most of the Bi-2212 suspensions have been fabricated using ethanol as the solvent.

In this work we report the suspension stability and rheological behaviour of ethanol-based Bi-2212 suspensions. The objective is to achieve the maximum solids loading in order to produce dense and good quality green tapes.

## 2. Preparation and characterization of Bi-2212 suspensions

### 2.1. Slurry preparation

A commercial powder composed by platelet shaped grains of stoichiometry $Bi_2Sr_2CaCu_2O_x$ (*Nexans Superconductors*, *Germany*) with a particle size distribution characterized by the parameters $d_{50} = 0.7\ \mu m$ and $d_{90} = 2.4\ \mu m$ and a surface area of $3.3\ m^2/g$ has been used. The density of the powder measured by He-picnometry was around $6.24\ g/cm^3$. Different solvents were tested as dispersing media, including polar and non-polar liquids. However, pure ethanol was the only one that produced stable and well-dispersed slips.[14,15] For this reason, ethanol (EtOH) of 99.5% purity (*Panreac*, *Spain*) has been selected as solvent in this study.

The slurry preparation process can be summarized as follows: in the first step, the dispersant was dissolved in a fixed volume of solvent and then, the Bi-2212 powder was added into this solution. In the second step, the mixture was homogenised with a high-energy ultrasounds probe (UP200S dr Hielscher, Germany) for 3 min until deagglomeration. Finally, the slurry was maintained under agitation with a magnetic stirrer. In order to perform the rheological characterization, a solid content of 15 vol.% (60 wt%) and a stirred time of 4 h was used. The same procedure has been used for sedimentation tests. However, in this case, the colloidal dispersion was prepared with 3 vol.% of solid content and stirred only for 10 min.

The research work started with the determination of the optimum dispersant concentration that produced stable slurries with optimized rheological properties. Concentrations of dispersant added to the slurries ranged from 0 to 1.1 wt% with respect to the powder content. Sorbitan Trioleate (*Sigma–Aldrich*, *Germany*), Glycerol Trioleate (*Sigma–Aldrich*, *Germany*) and Menhaden Fish Oil (*Dispersant*, *Z-3 from Richard E. Mistler*, *Inc.*, *USA*) were selected as dispersants. The first two dispersants can be considered as non-ionic surfactants with short chains and relatively low molecular weight, but capable to adsorb to the particles surfaces. For this reason, they have been considered as semisteric stabilizers, while the last one is a natural fish oil with polyunsaturated fatty acids that are considered to stabilize via steric hindrance.[16,17] The second part of the work studies the influence of solid content on the rheological properties of suspensions with optimum dispersant dosage.

### 2.2. Sample characterization

Rheological characterisation was carried out using a rheometer RS1 (Haake, Germany) with a double cone/plate sensor configuration (DC60/2°, Haake, Germany) that requires a sample volume of 5 ml and a testing temperature of $25 \pm 0.5\ ^\circ C$. The flow behaviour was measured using two different testing modes (controlled shear, CR, and controlled stress, CS). To obtain the high shear flow behaviour CR experiments were carried out by employing a measuring program with three stages; first a linear increase of shear rate from 0 to $1000\ s^{-1}$ in 3 min; a plateau at the maximum shear rate ($1000\ s^{-1}$) for 1 min, and decrease to zero shear rate in 3 min. The characterisation at the low shear rate region and the yield point determination were performed through CS experiment. In these measurements, shear stress is linearly increased until viscous flow occurs. The rheological behaviour of the slurries was fitted to regression models having two and four parameters, such as the Ostwald–de Waele and the Cross models, respectively.[18] The influence of the solid fraction on the slurry viscosity was studied considering the Krieger–Dougherty model[19] in order to predict the maximum solid loading to which the slips remain stable.

Sedimentation tests were carried out by filling the test tubes with the colloidal dispersions. The tubes were sealed and left undisturbed for a period of 680 h. At regular time intervals during this period, the sediment volumes were measured. The rate of sedimentation and the sediment packing efficiency were used as indicators of the colloidal stability.

The density of green pieces was measured by direct determination of the mass and volume and the values are reported as % of the theoretical density (TD) of Bi-2212 ($6.6\ g/cm^3$). The volume was calculated from the dimensions of green samples cut to a simple geometry.

Microstructural studies were performed using a JEOL 6400 SEM microscope equipped with an Energy Dispersive Spectroscopy (Link-Analytical EDS) system.

### 2.3. Analysis of slurry properties

#### 2.3.1. Influence of dispersant

The influence of the amount of dispersant was analysed using three different compounds: Sorbitan Trioleate (STO), Glycerol Trioleate (GTO) and Menhaden Fish Oil (MFO). First, the slurry

stability was evaluated by means of sedimentation experiments, $h(t)/h_0$, where $h(t)$ is the sedimentation front height at a given time and $h_0$ is the initial height. Fig. 1 shows the temporal evolution of $h/h_0$ during powder settling for different dispersant added amounts: STO (a), GTO (b) and MFO (c).

These measurements show that the suspension prepared without dispersant is the most stable because it exhibits the slowest settling rate regardless of the used dispersant. Moreover, it shows the highest settling density (the lowest final $h/h_0$ value), as compared with STO and MFO colloidal dispersions, and similar settling package than those prepared with GTO.

In addition, each dispersant induces a different behaviour. In the case of the sedimentation test of colloidal dispersions with STO, the greater is the STO content, the higher is the final $h/h_0$ value, and consequently, the lower is the settling packing density (Fig. 1a). Therefore, the STO seems to act as a poor dispersing agent in Bi-2212 ethanol-based suspensions in the range of studied concentrations. In the case of GTO (Fig. 1b), the final $h/h_0$ values, are similar to that obtained in the case of the suspension without dispersant, and near the same in all the analysed suspensions except in the case of the higher concentration. On the other hand, the use of the MFO leads to weakest dispersions stability because the Bi-2212 particles settle a few hours after having begun the sedimentation tests.

To explain these results, it is important to consider that the azeotropic mixture of methyl-ethyl ketone (MEK) and EtOH cannot provide the required stability and suspensions destabilize few minutes after having been prepared. Moreover, it was also impossible to prepare colloidal dispersions using toluene as solvent. Therefore, it is expected that Bi-2212 powders have a basic surface since the MEK and toluene are basic solvents.[20] On the other hand, EtOH is an acidic organic solvent and thus, proton exchange between the acid solvent and the basic particle surfaces would be effective.[21] Consequently, suspensions in EtOH are stable because of the high surface charge.

On the other hand, EtOH has a tendency to form hydrogen bonds and, hence, it has strong preference for oxidic particle surfaces. However, the addition of one of the studied dispersants to the colloidal dispersion produces a strong competitive adsorption between the EtOH and the dispersant at the particle surface. As a consequence, none of them are able to act as effective dispersing agent.

The effect of STO, GTO and MFO on the slurry viscosity in EtOH has also been studied. Fig. 2 shows the slurry viscosities at a constant shear rate of 100 $s^{-1}$ as a function of the dispersant content. The effect of each dispersant on the viscosity is also different. In the case of the STO and of the GTO, viscosity increases when the amount of dispersant increases, while MFO has a slight decrease at content of 0.6 wt% on a dry solid basis. This behaviour has been observed for all viscosity curves at any shear rate.

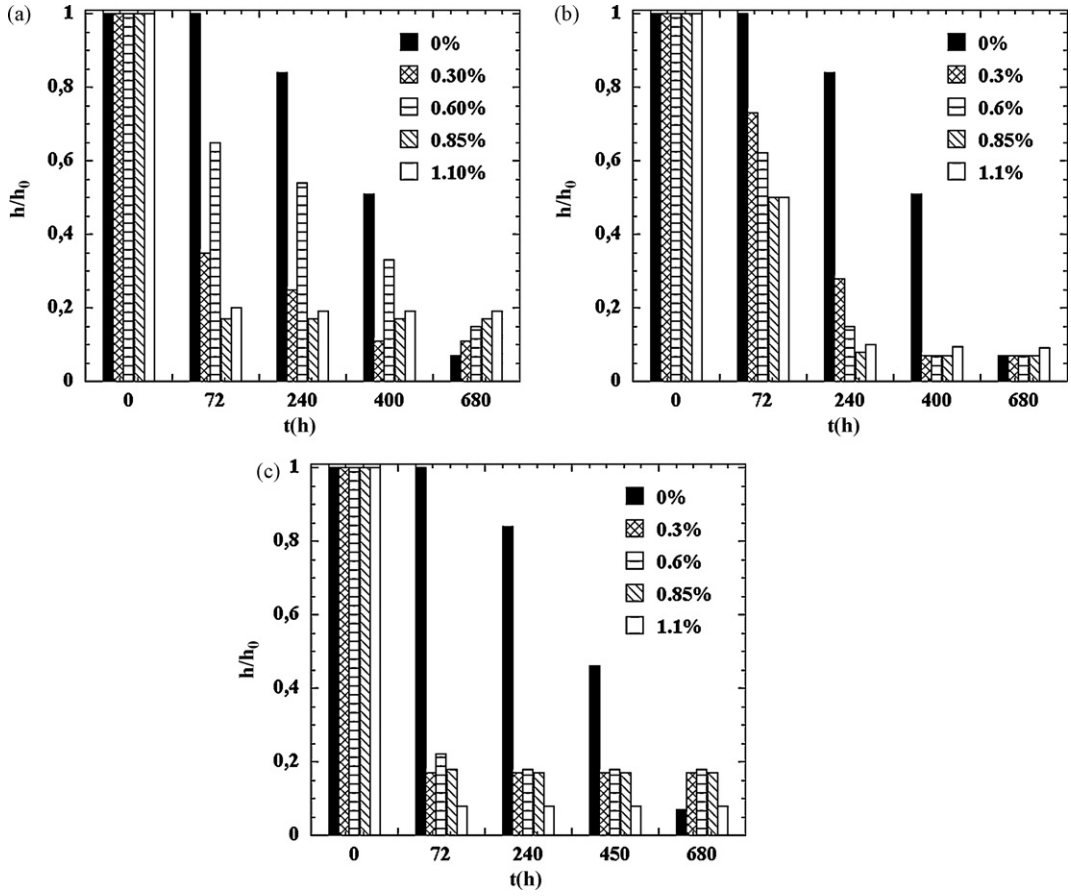


Fig. 1. Sedimentation tests for a 3 vol.% of Bi-2212 suspensions in EtOH as a function of different contents of STO (a), GTO (b) and MFO (c).

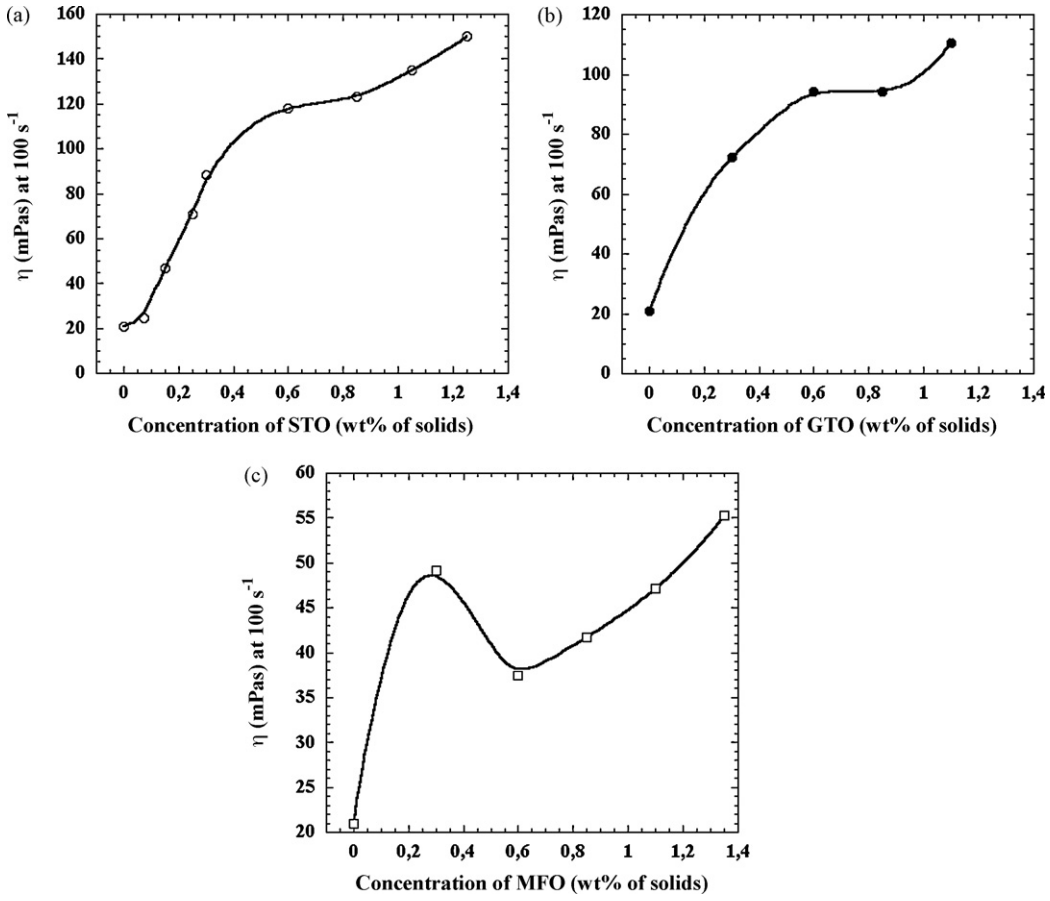


Fig. 2. Viscosity values Bi-2212 suspensions at 100 $s^{-1}$ as a function of the content of STO (a), GTO (b) and MFO (c).

These measurements also show that the best behaviour, associated with the lower viscosity values, is obtained for the suspension without dispersant. As a consequence, this suspension leads to the best degree of deagglomeration and the highest stability of particle suspension, following the same trend that was observed in the sedimentation experiments. It should be noticed that a careful choice of the dispersion system allows eliminating unnecessary additives in ceramic oxide dispersions such as the dispersant.[22] This fact is beneficial because of the difficulty in removing the dispersant from a green body, particularly if submicrometer-size particles are involved.

### 2.3.2. *Effect of solid loading*

A second important parameter to be determined is the maximum volume fraction of solid that can be dispersed in the suspension maintaining the flowability. According to the above results, this study has been performed using dispersant-free ethanol suspensions. For comparison purposes, suspensions with 0.85 wt% STO have also been studied. This dispersant content was the optimum one when the azeotropic mixture MEK/EtOH was used as the dispersion media.[15] Fig. 3 shows the dependence of the viscosity with the shear rate obtained in the CR mode as a function of solid content for suspensions without dispersant (a) and with 0.85 wt% STO (b). The plotted viscosity curves show shear-thinning flow behaviour in the studied shear region. This behaviour is due to shear-induced particle deagglomeration and alignment of the platelet-like particles, which allows the particles to slide past each other swelling more easily in the sheared fluid. As it is known, this behaviour is beneficial in the tape casting process because the slurry will display a lower viscosity under the shear of the blade. On the other hand, high viscosity values hinder particle motion and sedimentation during solvent evaporation process.

Viscosity curves of slurries with lower solid loads exhibit shear thickening flow behaviour at a moderate shear rate and, have not been presented in Fig. 3.

Another important point to mention is that for the whole solid contents bellow 70 wt%, viscosity values in the slurries without dispersant are lower than in the case of the solution with 0.85 wt% STO. By contrast, for a solid content of 75 wt% this relation is different, the slurry with STO exhibits slightly lower viscosity values in a wide range of shear rate values. However, this solid content is too high and suspensions properties are very sensitive to the processing conditions, leading to unstable slurries in some cases.

The flow behaviour has been characterized by the limit viscosity, $\eta_{Inf}$, which refers to the viscosity value extrapolated to infinite shear rate. These values were obtained from CR experiments by fitting the viscosity curves (Fig. 3) to the Cross model

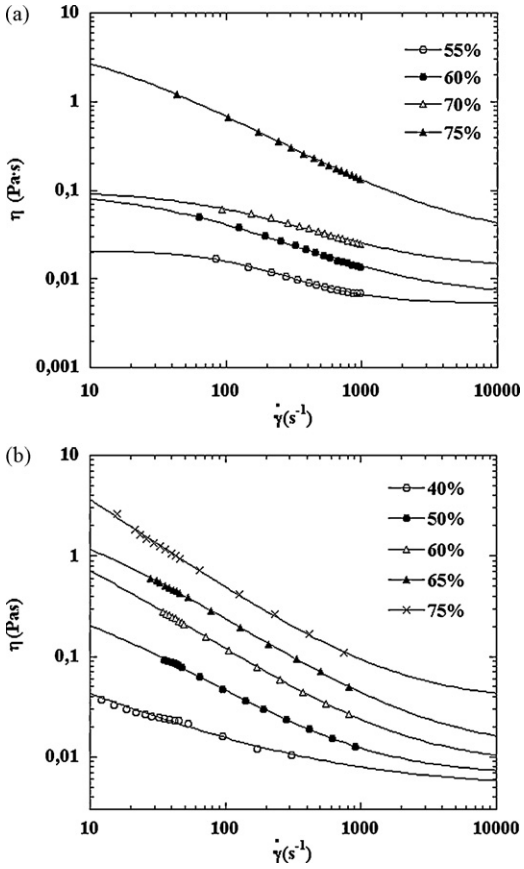


Fig. 3. Viscosity curves as a function of solid content for slurries without dispersant (a) and with 0.85 wt% STO (b). Solid lines correspond to the fitting of the experimental data to the Cross model.

(Eq. (1)) in the high shear region[18]:

$$\frac{\eta_0 - \eta}{\eta - \eta_{\mathrm{Inf}}} = (k\dot{\gamma})^m \tag{1}$$

where $\eta_0$ is the extrapolation of the viscosity to the zero shear rate and is referred to as zero shear viscosity, $\eta_{\mathrm{Inf}}$ is the limit viscosity, $\dot{\gamma}$ is the shear rate, $k$ is a constant with dimensions of time and $m$ is a dimensionless exponent.

The dependences of the limit viscosity values with the solid volume fraction ($\phi$) are plotted in Fig. 4 for both suspensions, with and without dispersant. These data were fitted to the Krieger–Dougherty model,[19] given by Eq. (2):

$$\eta = \eta_s \left(1 - \frac{\phi}{\phi_M}\right)^{-\phi_M[n]} \tag{2}$$

which allows the calculation of the maximum packing fraction ($\phi_M$), considered as the volume fraction of solids where the viscosity tends to infinity. In this equation, $\eta_s$ is the viscosity of the dispersing medium and $[\eta]$ is the intrinsic viscosity, which has a value of 2.5 for spherical particles and increases as sphericity decreases. It can be seen that the experimental data of both suspensions can be fitted to this model with the following fitting parameters: $\phi_M = 0.37$ and $[\eta] = 4.9$ for the slurry without dispersant and $\phi_M = 0.37$ and $[\eta] = 4.8$, in the other case. These values are consistent with the large aspect ratio of the platelet-like Bi-2212 particles. Applying the expression of Barnes,[23] $[\eta] = 3/10\,(L/e)$ and a shape factor value of 16.3 is obtained. The longitudinal dimension can be approximated to $L \sim d_{90} = 2.38\,\mu\mathrm{m}$, whereas the rheological properties are determined by the larger grains. Considering this approximation the platelet thickness has been estimated to be by 150 nm. This value is within the range of the measured by scanning electron microscopy of the superconducting grains (Fig. 5).

These theoretical predictions have been confirmed by slip casting concentrated suspensions in plaster moulds. In particular, suspensions with a solid content of 75 wt% were used. In the case of the suspensions without dispersant, a green density value of 37% of TD (2.47 g/cm$^3$) was obtained. This value coincides with the maximum solid loading obtained from viscosity experiments.

However, in the case of suspensions with 0.85 wt% STO, the green density value is slightly higher 39% of TD (2.57 g/cm$^3$). This is the expected behaviour taking into account the viscosity values presented in Fig. 3. This difference between this experimental value and the predictions of the Krieger–Dougherty model may be explained by introducing the concept of an effective volume that accounts for the volume occupied by the dispersant.[24]

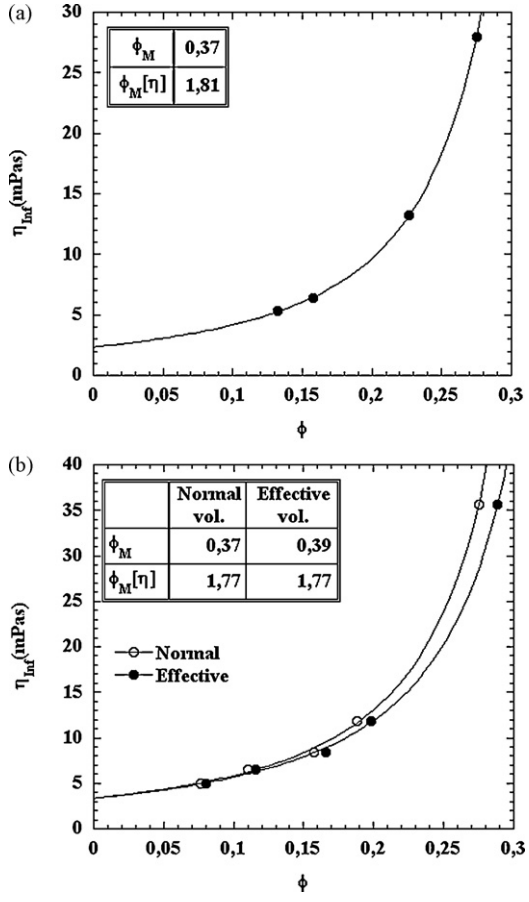


Fig. 4. Limit viscosity as a function of solid content for slurries without any dispersant (a) and with 0.85% ST (b). Solid lines correspond to the fitting of the experimental data to the Krieger–Dougherty model.

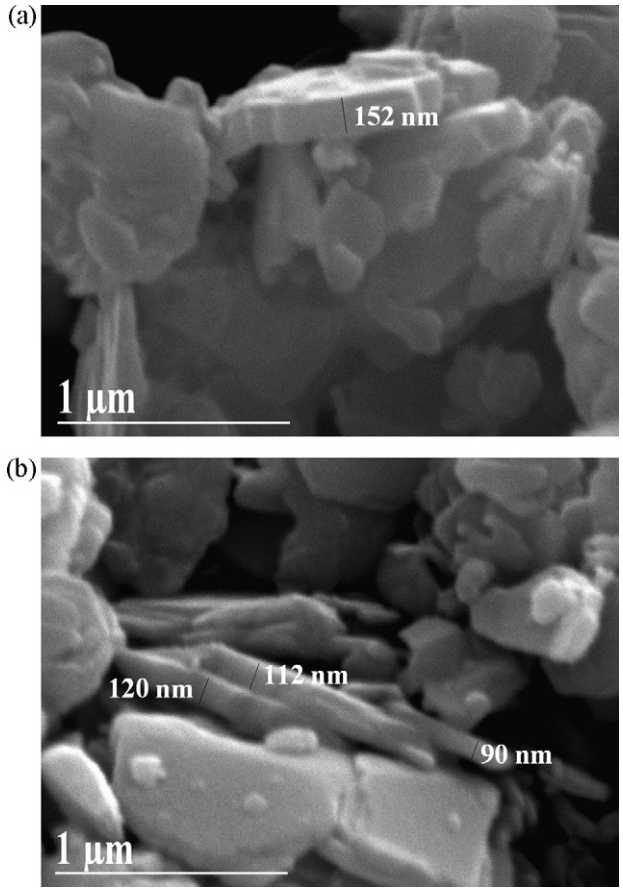


Fig. 5. SEM images of the superconducting Bi-2212 powder showing the plate-like form of particles. Thicknesses of some typical platelets are indicated.

The maximum fraction of solid has to be recalculated considering this effective volume concept, according to Eq. (3)[25]:

$$\phi_{ef} = \phi\left(1 + \frac{\rho_s S_s \Delta}{1000}\right) \quad (3)$$

where $\rho_s$ and $S_s$ are the density (in g/cm$^3$) and the specific surface area (in m$^2$/g) of the solid phase, and $\Delta$ is the thickness (in nanometers) of the adsorbed dispersant layer.

Considering the molecular structure of STO ($C_{60}H_{108}O_8$) with three lyophilic hydrocarbon chains, an interatomic distance C–C of 0.154 nm (16 bonds), a distance C=C of 0.134 nm (one double bond) and a carbon atomic radius of 0.077 nm[20], the maximum length of the hydrocarbon chains has been estimated to be around 2.68 nm. Taking $\rho_s = 6.24$ g/cm$^3$, $S_s = 3.3$ m$^2$/g and $\Delta = 2.68$ nm the volume fractions might be recalculated to provide the effective volume fraction, $\phi_{ef}$. Fig. 4b shows this new $\eta_{Inf}$ ($\phi$) dependence and the fit using the Krieger–Dougherty model. The obtained $\phi_{Mef}$ was determined as 0.39 that coincides with the green density for the specimen obtained from the 0.85 wt% STO slip.

## 3. Fabrication and characterization of Bi-2212 green tapes

### 3.1. Preparation of tape casting slips

These two different slurry compositions were used for tape casting. The quantity of each component that is required for preparing 150 g of tape casting slips is presented in Table 1. Suspensions were prepared by adding the Bi-2212 powder to the solvent containing the dispersant, when needed, and subsequently subjected to deagglomeration by a high-energy ultrasonic mixing for 3 min. Then, the slurry was mixed in a centrifugal ball mill (Retsch S100, Germany) with polycarbonate balls for 4 h. A solid content of 22 vol.% (70 wt%) was fixed at this step. Finally, the plasticizer and binder were added to the Bi-2212 suspension. This mixture was ball milled again for 2 h.

### 3.2. Rheological characterization of tape casting slips

During the fabrication process, rheological properties of the suspensions were monitored as a quality control. Fig. 6 shows the viscosity curves before and after the addition of binder and plasticizers. As it is expected, suspensions with binder are more viscous than those without binder, but, the binder addition leads to the transition from significant shear-thinning to nearly Newtonian flow behaviour. Appling the Ostwald–de Waele power law, given by Eq. (4):

$$\eta = K\dot{\gamma}^{n-1} \quad (4)$$

where $K$ is the flow consistency index and $n$ is the flow behaviour index, the viscosity curves can be described using the fitting parameters whose values are shown in Fig. 6. It is clearly observed that the degree of shear-thinning decreases from $n \sim 0.24$ for the slips before adding the binder to $n \sim 0.90$ for the

Table 1
Slurry compositions.

| | Component | 0.85% STO | | Without dispersant | |
|---|---|---|---|---|---|
| | | wt% | g | wt% | g |
| Powder | Bi-2212 | 62 | 93 | 62 | 93 |
| Dispersant | Sorbitan Trioleate | 0.53 | 0.79 | 0 | 0 |
| Binder | Polyvinyl Butyral B79 | 5.80 | 8.71 | 5.80 | 8.71 |
| Plasticizer I | Bibutyl Phthalate | 2.90 | 4.36 | 2.90 | 4.36 |
| Plasticizer II | Polyalkylene Glycol | 2.90 | 4.36 | 2.90 | 4.36 |
| Solvent | Ethanol | 25.87 | 38.78 | 26.40 | 39.57 |
| Total | | 100 | 150 | 100 | 150 |

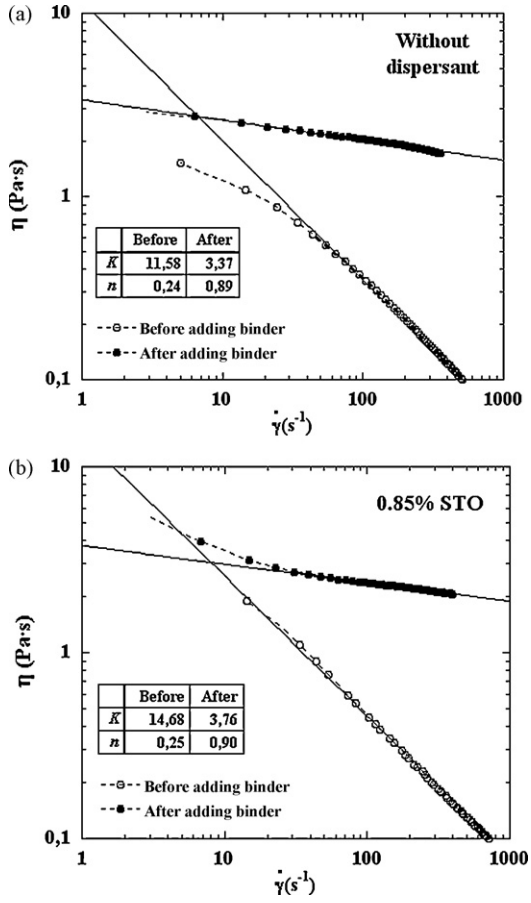


Fig. 6. Viscosity curves of the slips before and after adding both the binder and the plasticizer. Slip without dispersant (a) and with 0.85 wt% of STO (b). The continuous solid lines show the Ostwald–de Waele fits.

binder containing slurries ($n = 1$ corresponds to ideal Newtonian fluid).

Although the main feature to consider at this stage is that the film has to be consistent and with good resistance to cracking during drying, rheological tests can be also used to identify the range of stresses for which viscous flow occurs, i.e. the yield point. As already noted, the measurements in CS mode are most appropriate for obtaining this information. In our case, CS testing mode has been performed up to a stress value of 20 Pa. Fig. 7 shows the behaviour of the slip deformation against the applied stress. For each sample there are two lineal regions, whose intercepting point defines the yield point.[25] It can be seen that in the suspension without dispersant the viscous flow regime starts at lower stress value (around 1 Pa) than in the suspension with 0.85 wt% STO, where this transition takes place at 13 Pa. This means that, when the particles are at rest, the slip with 0.85 wt% STO has a higher tendency to form structures than in the other dispersant-free slurry.

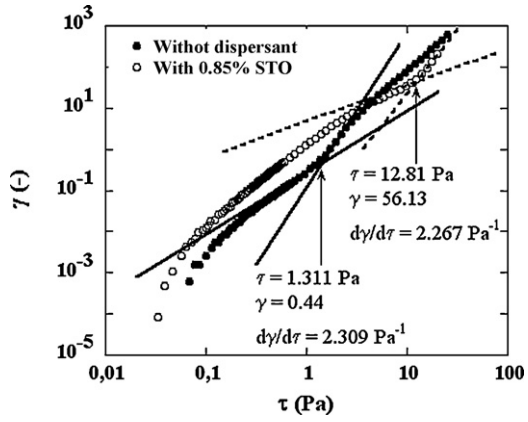


Fig. 7. Yield point determination. Log–log representation of the slip deformation ($\gamma$) as a function of the shear stress performed in CS mode.

### 3.3. Morphology of Bi-2212 green tapes

Once it is verified that slurry has adequate rheological properties, it is degassed and the suspension is ready for the green tape fabrication. Tape casting was carried out onto Silicone Coated Mylar film on a fixed gap doctor blade system (doctor blade assemblies made by *Richard E. Mistler*, *Inc.*). A casting velocity of 20 mm/s and a gap height of 200 μm were selected as the casting parameters ($\dot{\gamma} = 100\,s^{-1}$). Drying of the ceramic tapes was performed at room temperature.

Both tapes, which have been cast with the above conditions, are flat, homogeneous in thickness and have not macroscopic surface irregularities. The dimensions that have been reached are 60 cm × 10 cm. The tape manufactured with the slip without dispersant shrank to about 32% in the thickness direction, while that one manufactured from the slip with 0.85 wt% STO shrank to about 27%. Fig. 8 shows SEM micrographs of a cross-sectional fracture (a and c) and of the top surfaces (b and d) of both processed tapes without and with dispersant, respectively. As can be observed in these SEM images, the tape without dispersant is slightly thinner than the tape with 0.85% STO. This indicates that, under similar processing conditions, particles are better packed in the tape prepared from the slip without dispersant. This assertion is corroborated by the calculated green density values collected in Table 2.

Looking at the surface microstructures (Fig. 8b and d) it can be observed that a lower porosity and a greater particle surface compaction have been reached in the tape fabricated from the suspension without dispersant. Making a quantitative analysis of

Table 2
Properties of green and sintered tapes.

| | Before sintering | | After sintering | |
|---|---|---|---|---|
| | Thickness (μm) | Density (g/cm$^3$)–% to TD | Thickness (μm) | Density (g/cm$^3$)–% to TD |
| Without dispersant | 135 | 3.24–49.0% | 118 | 3.04–46.1% |
| With 0.85% of STO | 145 | 2.96–44.8% | 138 | 2.74–41.5% |

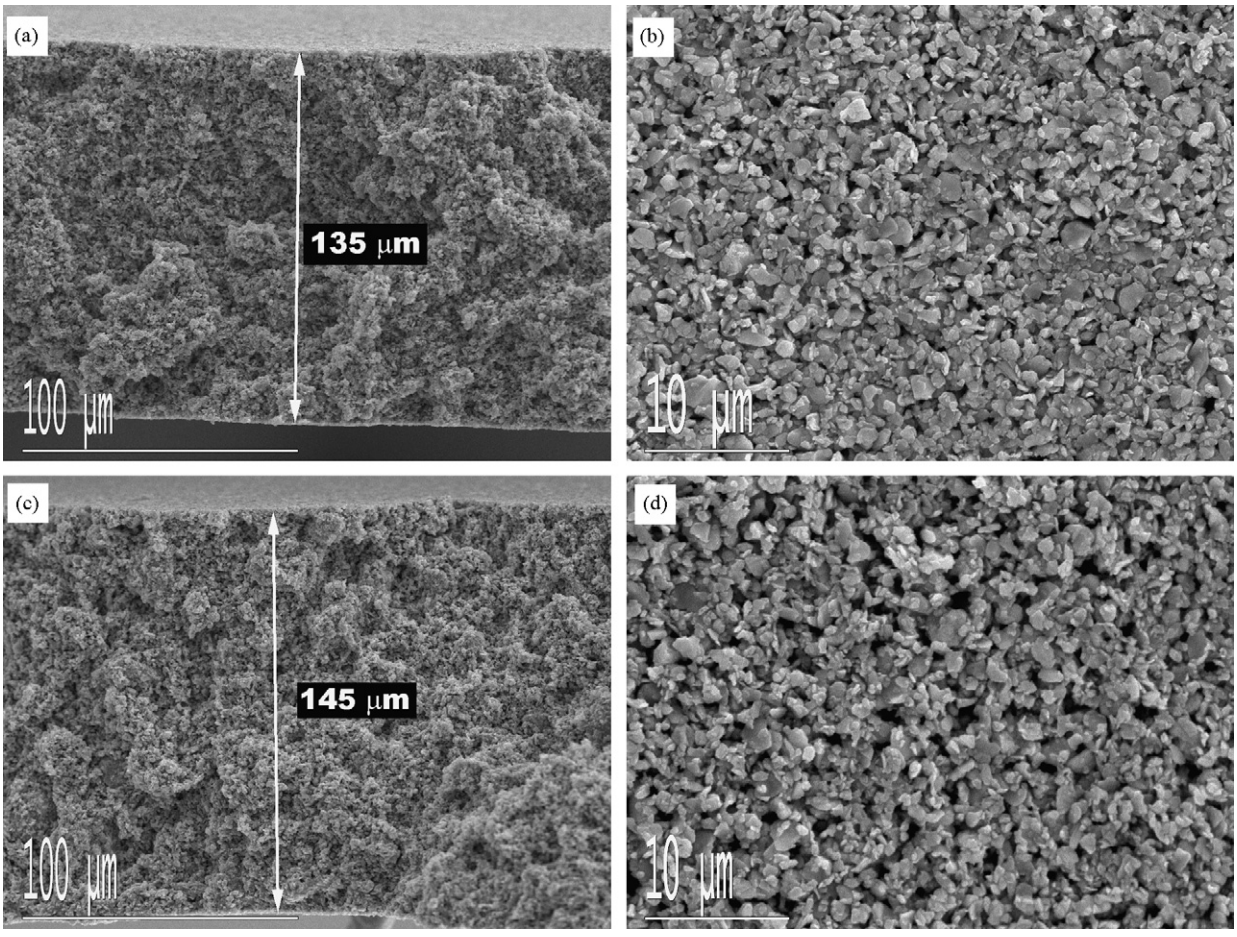


Fig. 8. SEM micrographs of cross-sectional fracture (a and c) and top surface (b and d) of green sheets. (a and b) Correspond to the tape fabricated without dispersant and (c and d) to the tape with 0.85 wt% STO.

the porous surface, by difference image contrast and using the software analysis of Digital Micrograph Gatan Inc., a porosity of 23.5 and 36% are obtained in the films without dispersant and with a 0.85 wt% STO, respectively.

An identical sintering treatment has been used for both tapes, avoiding the formation of liquid phases. The thermal decomposition of organic additives occurs at 400 °C, as determined by differential scanning calorimetric and thermal gravimetric analysis. Therefore, the binder burnout of the green sheets took place between room temperature and 400 °C at a heating rate of 16 °C $h^{-1}$. After binder removal, the samples were heated up to 865 °C at a rate of 300 °C $h^{-1}$. Samples were held at this temperature for 2 h and, finally, they were cooled at room temperature.

After this thermal treatment, sintered specimens were obtained with the microstructures shown in Fig. 9 and the characteristics listed in Table 2. SEM images show that the thickness of the film obtained from the suspension without dispersant was reduced by a 10%, while in the film obtained with 0.85 wt% STO this reduction is about a 5%. By contrast, the surface porosity has increased considerably, from 33.2 to 48.8% when adding STO. In relation to these results, it is clear that, the superconducting materials based on Bi-2212 usually do not densify by usual sintering heat treatment (without the assistance of the liquid phases) and the density even decreases as demonstrated in a previous work.[26] According to the density values shown in Table 2, after the sintering thermal treatment, the sheet obtained from the slip without dispersant leads to samples with a higher density than in the case of the suspension with STO.

## 4. Fabrication of textured superconducting coatings

Due to the advantage of fabricating tapes without dispersant; it has been explored whether it is possible to obtain superconducting coatings using these sheets. For this reason, five pieces cut from green tapes without dispersant were placed on a silver plate and laminated via cold compression by applying 50 MPa of pressure. After having performed the initial heat treatment to eliminate all the additives, sample was textured using a Laser Melting Zone (LMZ) process with a high power diode laser.[7] The laser beam is focused in a thin line, inducing the melting of a small sample volume. In order to reduce the porosity, the process has been performed in three steps; while the sample support temperature was keep at 650 °C. In the first one the sample was moved with a traverse rate of 1000 mm $h^{-1}$, in the second one at 500 mm $h^{-1}$ and finally, texture was reached at 30 mm $h^{-1}$ using the same linear power density of 1.5 W $mm^{-1}$. Due to the incongruent melting of Bi-2212 materials, an additional heat treatment (60 h at 850 °C and 12 at 800 °C in air) has

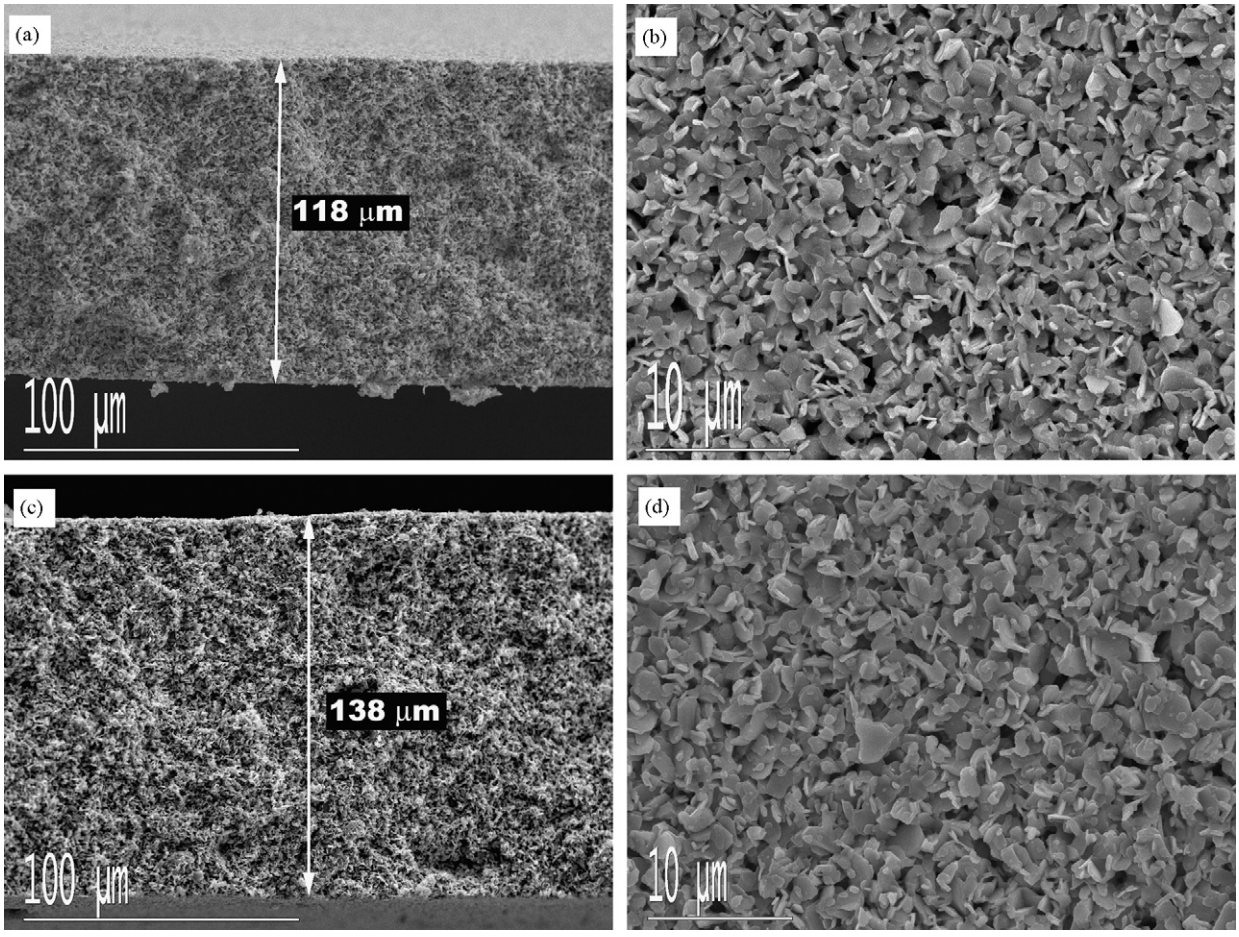


Fig. 9. SEM micrographs of a cross-sectional fracture (a and c) and top surface (b and d) of the sintered sheets. (a and b) Without dispersant and (c and d) with 0.85 wt% STO.

to be performed after processing in order to recover the adequate superconducting phase.

The thickness of the final sample is 450 μm, approximately a 60% of the green tape thickness, and in accordance with the densification that takes place during LZM, reaching density values of near the 85% of the theoretical density in the textured material. According to the microstructural analysis the superconducting Bi-2212 is the main phase within this processed material, however, some grains of the $Bi_2Sr_2CuO_x$ and $(SrCa)CuO_2$ secondary phases can also been observed. In addition silver grains have been observed inside the superconducting coating, although no silver diffusion inside the superconducting grains was detected.

Superconducting properties have been characterized by measuring the temperature dependence of the ac susceptibility (amplitude of 1 Oe and frequency of 1 Hz) and the magnetic field dependence magnetization at 5 K in a SQUID magnetometer (MPMS-55 Quantum Design). Transport critical current density values ($J_c$) have also been measured at 77 K using a four-point configuration.

From the ac susceptibility measurements it has been deduced that the critical temperature, defined as the temperature at which the in-phase component reaches a value of $0.001\chi'$ (5 K), is 88.5 K. A relevant fact is that a small diamagnetic signal appears at temperatures bellow 110 K showing that a small amount of the $Bi_2Sr_2Ca_2Cu_3O_x$ high $T_c$ phase (Bi-2223) is also generated in the textured sample.

The evolution of the irreversible magnetization with magnetic field at 5 K shows a potential dependence, $M_{irr} \approx H^{-q}$, with an exponent of 0.41, as it was obtained in Bi-2212 textured thin rods.[27] However, the critical current density at 77 K was only 300 A $cm^{-2}$, considering the total section of the superconducting coating. This value is approximately a 25% of the best previous results that have been obtained in samples with a similar thickness and processed with the same parameters, but with a precursor powder whose grain size distribution was characterized by $d_{50} = 11.6$ μm, a value that is 16 times the value of the powder used in the present study.[7,15] This superconducting behavior shows that the best processing parameters used for a precursor powder of $d_{50} = 11.6$ μm are not adequate if the powder size is reduced to $d_{50} = 0.7$ μm. A similar behavior was also observed in LZM textured Bi-2212 thin rods, where the $J_c$ values were reduced to a 25% of the optimum ones when the superconducting precursor powder was changed.[28] This result can be understood considering the different physical transformations that take place during the melt of these multiphase materials. The optimum processing parameters of the LZM technique are strongly dependent on the precursor characteristics and an optimization process is required to obtain the adequate

processing values. Due to the good results that were obtained in Bi-2212 thin rods, simplex optimization methods[28] are being used to improve these superconducting materials. As a conclusion of all these experiments, it can be deduced that it is possible to obtain superconducting Bi-2212 coatings using the colloidal route without dispersant.

## 5. Conclusions

The dispersion of Bi-2212 powders in EtOH-based solvent using triglycerides and oils like Sorbitan Trioleate, Glycerol Trioleate and Menhaden Fish Oil as dispersants, has been studied by measuring the rheological behavior of suspensions and the sedimentation behaviour. It has been found that the use of pure EtOH as a solvent allows stabilizing the Bi-2212 suspensions without the addition of any dispersant. This result serves to reduce the amount of residual organic impurity in the tapes by eliminating unnecessary additives that deteriorate the transport superconducting properties. In addition, it also simplifies the slurry formulation leading to economical benefits.

It is expected that the suitable combination of the acidic nature of EtOH and the basic sites at the Bi-2212 particle surface, coupled with an efficient action of high-energy ultrasound mixing is sufficient to obtain a stable and well-dispersed slip, up to a solid content around 22 vol.% (70 wt%). The stabilization without dispersant demonstrates that electrostatic charging is the effective mechanism operating for Bi-2212 particles dispersed in a polar organic solvent like EtOH.

It has been also found that the maximum packing fraction was around 37 and 39 vol.% for slip with and without dispersant, respectively. These values were consistent with the measured density of concentrated slip cast samples.

Tapes obtained by casting EtOH-based suspensions without dispersant show suitable properties such as strength and flexibility. Tape density obtained from the slip without dispersant is higher than that fabricated from the slip with 0.85 wt% STO. After sintering, such difference remains.

Tapes without dispersant have been used to fabricate superconducting coatings on silver substrates with critical temperatures close to 90 K. Results show that due to the reduction of the powder size, the processing parameters have to be optimized again in order to recover the best superconducting properties that were previously obtained in these materials using precursors with bigger grain size.

## Acknowledgement

This work was supported by the Spanish Science and Innovation Ministry (Project MAT2008-05983-C03-01).

## References

1. Song Y, Zhao L, Li P, Qu T, Huang Y, Han Z. The preparation and characterization of Bi-2212 film on Ag substrate by dip-coating method. *Physica C* 2006;**442**:134–8.
2. Ilyushechkin AY, Yamashita T, Mackinnon IDR. Re-melting of Bi-2212/Ag laminated tapes by partial melting process. *Physica C* 2002;**377**:362–71.
3. Koo J-W, Lee SY, Kim HD, Ha KH, Ahn JH, Chung YS, et al. Fabrication of Bi-2212/Ag superconducting tape using a screen-printing method. *J Mater Sci* 1994;**29**(17):4639–44.
4. Köbel S, Schneider D, Sager D, Sütterlin P, Fall L, Gauckler LJ. Processing and properties of $Bi_2Sr_2CaCu_2O_x$ thick films on polycrystalline magnesium oxide substrates. *Physica C* 2003;**399**:107–19.
5. Lang Th, Buhl D, Schneider D, Al-Wakeel S, Gauckler LJ. Texture in melt-processed Bi-2212. *J Electroceram* 1997;**1**(2):133–44.
6. Huang SL, Dew-Hughes D, Zheng DN, Jenkins R. Effects of MgO addition on phase evolution and flux pinning of Bi-2212/Ag tapes fabricated by electrophoretic deposition and partial-melting processing. *Supercond Sci Technol* 1996;**9**:368–73.
7. Mora M, Gimeno F, Angurel LA, de la Fuente GF. Laser zone melted $Bi_2Sr_2CaCu_2O_8$ thick films on (1 0 0) MgO substrate. *Supercond Sci Technol* 2004;**17**:1133–8.
8. Levinson M, Shah SSP, Wang DY. Laser zone-melted Bi–Sr–Ca–Cu–O thick films. *Appl Phys Lett* 1989;**55**:1683.
9. Buhl D, Lang T, Gauckler LJ. Critical current density of Bi-2212 thick films processed by partial melting. *Supercond Sci Technol* 1997;**10**: 32–40.
10. Kase J, Morimoto T, Togano K, Kumakura H, Dietderich DR, Maeda H. Preparation of the textured Bi-based oxide tapes by partial melting process. *IEEE Trans Mag* 1991;**27**:1254–7.
11. Zhang W, Hellstrom EE. The development of aligned microstructure during melt processing of Bi-2212 doctor blade films. *Physica C* 1993;**218**:141–52.
12. Ilyushechkin AY, Yamashita T, Boskovic L, Mackinnon IDR. The effect of Yb addition in $Bi_2Sr_2Ca_{1-x}Yb_xCu_2O_y$ partial melted thick films. *Supercond Sci Technol* 2004;**17**:1201–8.
13. Alarco JA, Ilyushechkin AY, Yamashita T, Bhargava A, Barry J, Mackinnon IDR. Microstructural investigation of Bi–Sr–Ca–Cu-oxide thick films on alumina substrates. *J Mater Sci* 1997;**32**:3759–64.
14. Mora M, Lennikov V, Amaveda H, Angurel LA, de la Fuente GF, Bona MT, et al. Fabrication of superconducting coatings on structural ceramic tiles. *IEEE Trans Appl, Supercond* 2009;**19**:3041–4.
15. F. Gimeno, Fabricación y caracterización de materiales superconductores de alta temperatura con geometrías que permitan grandes longitudes para su uso en limitadores de corriente. PhD Thesis. University of Zaragoza; 2009.
16. Mistler RE, Twiname ER. *Tape casting: theory and practice*. Westerville, OH: The American Ceramic Society; 2000.
17. Moreno R, Córdoba G. Oil-related deflocculants for tape casting slips. *J Eur Ceram Soc* 1997;**17**:351–7.
18. Cross MM. Rheology of non-Newtonian fluids: a new flow equation for pseudoplastic systems. *J Colloid Sci* 1965;**20**(5):417–37.
19. Krieger IM, Dougherty TJ. A mechanism for non-Newtonian flow in suspensions of rigid spheres. *Trans Soc Rheol* 1959;**3**:137–52.
20. Lide DR, editor. *C.R.C. Handbook of Chemistry and Physics*. 84th ed. Boca Raton: C.R.C. Press; 2003.
21. Boschini F, Rulmont A, Cloots R, Moreno R. Rheological behaviour of $BaZrO_3$ suspensions in non-aqueous media. *Ceram Int* 2008;**35**:1007–13.
22. Parish MV, Garcia RR, Bowen HK. Dispersions of oxide powders in organic liquids. *J Mater Sci* 1985;**20**:996–1008.
23. Barnes HA, Hutton JF, Walters K. *An introduction to rheology*. Elsevier Science; 1989.
24. Gutierrez CA, Moreno R. Interparticle potentials in nonaqueous silicon nitride suspensions. *J Am Ceram Soc* 2003;**86**:59–64.
25. Gutiérrez CA, Sánchez-Herencia AJ, Moreno R. Plástico o pseudoplástico? Métodos de determinación y análisis del punto de fluidez de suspensiones cerámicas. *Bol Soc Esp Ceram Vidr* 2000;**39**:105–18.
26. Johnson Jr DW, Rhodes WW. Retrograde densification in $Bi_2Sr_2CaCu_2O_8$ superconductors. *J Am Ceram Soc* 1989;**72**:2346–50.
27. Martínez E, Angurel LA, Díez JC, Navarro R. Analysis of the length scales in the induced critical currents of $Bi_2Sr_2CaCu_2O_{8+\delta}$ thick fibres. *Physica C* 1997;**289**:1–21.
28. Natividad E, Díez JC, Angurel LA, Andrés JM. Successful application of simplex methods to the optimization of textured superconducting ceramics. *J Am Ceram Soc* 2004;**87**:1216–21.